RSC Advances

PAPER

View Article Online
View Journal | View Issue

Cite this: *RSC Adv.*, 2018, **8**, 5151

In vivo analysis of the effects of CoCrMo and Ti particles on inflammatory responses and osteolysis

Juehong Li,† Yamin Li,† Xiaochun Peng, Bin Li, Hui Qin and Yunsu Chen *

Received 10th November 2017
Accepted 23rd January 2018

DOI: 10.1039/c7ra12325f

rsc.li/rsc-advances

Metal wear particles play a major role in periprosthetic osteolysis and aseptic loosening in patients with total joint arthroplasty. The ability to induce osteolysis depends on the size, shape, dose, and type of the particles. However, much remains unknown regarding which type of metal particles are most reactive. We compared the inflammatory response and bone loss induced by two metal wear particles, cobalt–chromium–molybdenum (CoCrMo) and titanium (Ti), in a mouse calvaria model of osteolysis. We found that CoCrMo particles caused markedly greater bone resorption than Ti particles, according to three-dimensional images of the calvariae. CoCrMo particles activated more functional osteoclasts by significantly increasing the expression of the osteoclast-specific gene tartrate-specific acid phosphatase (Trap), calcitonin receptor (Ctr), and nuclear factor of activated T cells c1 (Nfatc1), and induced a greater increase in the ratio of receptor activator of nuclear factor kappa B ligand (RANKL)/osteoprotegerin (OPG) than Ti particles. CoCrMo particles also induced a stronger local inflammatory response, markedly increasing the expression and secretion of tumor necrosis factor-α and interleukin-1β compared with Ti particles. Therefore, CoCrMo particles induced a more severe inflammatory response and greater osteolysis than Ti particles *in vivo*.

1 Introduction

Total joint arthroplasty (TJA) is an efficient treatment for patients with end-stage joint diseases such as osteoarthritis, femoral head necrosis, and rheumatoid arthritis. Because it relieves pain and allows functional recovery, TJA has become increasingly popular in older adults and even young people. The annual number of operations is increasing rapidly worldwide.[1,2] However, regardless of the highly satisfactory overall results, complications resulting in surgical revision also occur. It has been confirmed that wear particle-induced inflammatory osteolysis is still the main reason for TJA failure and joint revision.[3–5] This complication is a macrophage-based inflammatory response to wear particles generated regionally at implant interfaces, and the lifetime of a joint prosthesis has been convincingly shown to depend on the type and amount of implant debris.[6–8]

The effect of wear particles on periprosthetic osteolysis is mainly associated with the dose, size, shape, and type of wear particle.[9–12] It is generally recognized that only particles of <10 μm in diameter induce an inflammatory response *in vitro*.[13–15] Sabokbar *et al.*[16] demonstrated that particle-induced osteoclast formation and bone loss are not significantly affected by the particle shape, but by the contact between cells and the particles. According to previous studies,[9,10,14] smaller particles induce a stronger inflammatory reaction than larger particles. However, the specific types of particle, which are maximally inflammatory and induce osteolysis *in vivo*, remain unclear.

Several kinds of wear particles warrant continuous investigation, including ultra high molecular weight polyethylene (UHMWPE), polymethyl methacrylate (PMMA), cobalt–chromium–molybdenum (CoCrMo), and titanium (Ti) particles. With the application of highly cross-linked polyethylene and ceramic liners, and the widespread popularity of the cementless fixation concept, the clinical complications caused by UHMWPE and PMMA particles are expected to be resolved at the material level.[17–19] However, metal particles remain as a lingering problem. Several clinical studies have reported high rates of prosthetic loosening and revision in patients with metal-on-metal joint prostheses made of CoCrMo and Ti alloy.[20–22] Therefore, we focused on the osteolysis-inducing effects of CoCrMo and Ti particles.

In this study, we investigated the effects of CoCrMo and Ti particles on the release of proinflammatory cytokines and osteolytic bone loss in a mouse calvarial model. To perform a side-by-side comparison, we implanted equal doses of the two particle types into mouse calvariae for 2 weeks and then examined the local inflammatory reaction and osteolysis in the calvariae by scanning electron microscopy, micro-computed tomography (micro-CT), histochemical and immunochemical staining, and molecular biology methods.

Department of Orthopaedic Surgery, Shanghai Jiao Tong University Affiliated Sixth People's Hospital, Shanghai, China. E-mail: yschen2016@hotmail.com; Fax: +86-21-24058102

† These authors contributed equally to this work.

2 Materials and methods

2.1 Particle preparation

Commercial Ti particles were purchased from Johnson Matthey Chemicals (#00681, Ward Hill, Massachusetts, USA). According to the product specifications, 90% of the Ti particles were <3.6 μm in diameter and the mean diameter was 2.93 μm. CoCrMo particles, a kind gift from Sandvik (Stockholm, Sweden), had a mean diameter of 2.77 μm (range: 0.02–11.57 μm). The sizes and shapes of the particles were determined by a scanning electron microscope (Vega 3 LMU, Tescan, Brno, Czech Republic) (Fig. 1A and B). The particles were washed several times with 75% ethanol and tested negative for endotoxin with a commercial Limulus Amebocyte Lysate Assay Kit (Bio-Whittaker, Walkersville, MD, USA), as described previously.[23,24]

2.2 Animals and grouping

All animal procedures were performed in compliance with the guidelines for care and use of Laboratory Animals of Shanghai Jiaotong University and approved by the Institutional Animal Care and Use Committee of Shanghai Jiaotong University Affiliated Sixth People's Hospital. Healthy 8–10 week-old male BALB/c mice ($n = 96$) were equally and randomly divided into three groups: control group (sham surgery and phosphate-buffered saline [PBS]), CoCrMo particle group (surgery and 20 mg per mouse CoCrMo particles), and Ti particle group (surgery and 20 mg per mouse Ti particles).

2.3 Calvarial osteolysis model

The mouse calvarial osteolysis model was established as described previously.[25] Briefly, the mice were anesthetized by an intraperitoneal injection of 90 mg kg^{-1} 4% chloral hydrate. A longitudinal 1 cm incision was made on the mouse head and the periosteum was separated from the skull raphe by sharp dissection. In Ti and CoCrMo particle groups, 20 mg Ti or CoCrMo particles were embedded into the surfaces of the bilateral parietal bones, whereas in the control, the wounds were sutured and injected with 20 mg PBS. Penicillin (10 000 U) was injected intraperitoneally daily for 3 days after surgery. After 2 weeks, the mice were sacrificed by an overdose of anesthetic, and calvariae were harvested for analyses.

2.4 Micro-CT imaging

Formalin-fixed calvariae ($n = 8$ per group) from each group were scanned by a micro-CT scanner (SkyScan1176, version 1.1 software [build 6]; Bruker, Kontich, Belgium) at 9 mm isometric intervals with X-ray energy settings of 80 kV and 80 mA, and an exposure time of 100 ms, as described previously.[26,27] The wear particles were cleared before scanning to avoid metal artifacts.[28] The scanned images of each sample were reconstructed into three-dimensional (3D) images at the same thresholds with NRecom software (version 1.6.9.8). A region of interest (ROI) of 3 × 3 mm^2 with the midline suture at its center was located in each scanned image and combined to form a volume of interest (VOI) of 3 × 3 × 1 mm^3, as described previously.[26,27] Bone mineral density (BMD), the bone volume/tissue volume ratio (BV/TV), total porosity, and number of pores in the VOI were evaluated by CT Analyzer software (version 1.15.4.0+, Bruker).

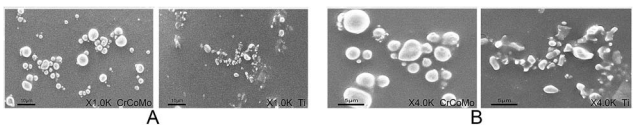

Fig. 1 Characteristics of Ti and CoCrMo particles. Representative scanning electron micrographs of CoCrMo and Ti particles at magnifications of (A) ×1000 and (B) ×4000.

2.5 Bone histomorphometry

Samples ($n = 8$ per group) from each group were fixed in 50 ml formalin solution for 48 h, decalcified with 50 ml of 10% EDTA for 14 days, dehydrated, and embedded in paraffin. Sections (6 μm thick) of each sample were obtained in the coronal plane within the ROI. The sections were stained with hematoxylin and eosin (HE), and imaged with a high quality light microscope focusing on the midline suture. The histomorphology and eroded surface area of each sample were evaluated by Image-Pro Plus software 6.0 (Media Cybernetics, Bethesda, MD, USA), as described previously.[27]

To detect osteoclasts, the sections were stained with a commercial tartrate-specific acid phosphatase (TRAP) kit. The number of TRAP-positive multinucleated osteoclasts represented as dark red-stained granules within the edge of the resorption lacuna was determined in the sections, as described previously.[26,27] The osteoclast surface per bone surface (OcS/BS, %) was determined in each sample using Image-Pro Plus software 6.0, as described previously.[29]

To immunohistologically stain the sections, they were dewaxed and antigens were retrieved in sodium citrate prior to overnight incubation at 4 °C with a primary antibody. After washing, the sections were incubated with an appropriate secondary antibody for 30 min. Staining was developed with diaminobenzidine. The sections were then washed and counterstained with hematoxylin. The primary antibodies used were anti-tumor necrosis factor α (TNF-α) (Abcam, Shanghai, China), anti-interleukin 1β (IL-1β) (Abcam), anti-IL-6 (Abcam), and anti-receptor activator of nuclear factor kappa B ligand (RANKL) (Abcam).

2.6 Real-time quantitative PCR

Calvariae ($n = 8$ per group) were lysed in TRIzol Reagent (Invitrogen, Paisley, UK), and total RNA was extracted with an RNeasy Kit (Qiagen, Valencia, CA, USA), as described previously.[25] cDNA was synthesized from the purified RNA by reverse transcription (RT) and analyses were performed as described previously.[25,26] The housekeeping gene glyceraldehyde 3-phosphate dehydrogenase (Gapdh) was used as the internal reference to normalize the target gene levels. All measurements were performed in triplicate. The primers used in this study are shown in Table 1.

Table 1 Details of the primers used for RT-PCR

Genes	Forward (5′–3′)	Reverse (5′–3′)
TRAP	TTATTGAATAGCAGTGACAG	AAATCACTCTTTAAGACCAG
CTR	ACCGACGAGCAACGCCTACGC	GCCTTCACAGCCTTCAGGTAC
CK	ACGGAGGCATTGACTCTGAA	CACTGCTCTCTTCAGGGCTT
NFATc1	GGCTGCCTTCCGTCTCATAGT	CAACGCCCTGACCACCGATAG
GAPDH	GAGAAGGCTGGGGCTCATTT	CCAATATGATTCCACCCATG

2.7 Enzyme-linked immunosorbent assays (ELISAs) of cultured calvariae

Calvariae ($n = 8$ per group) of all mice were collected, randomly distributed into the wells of a 12-well plate, and incubated in 1.5 ml Dulbecco's modified Eagle's medium with 1% penicillin and streptomycin for 24 h at 37 °C with 5% CO_2. The culture medium was collected and analyzed by ELISAs to measure TNF-α, IL-1β, IL-6, RANKL, and osteoprotegerin (OPG), as described previously.[28]

2.8 Statistical analysis

Data are presented as means ± standard deviations. All values were first evaluated by the Kolmogorov–Smirnov test to ensure their normality and homogeneity of variance. One-way analysis of variance was used to perform multiple comparisons and a two-sided Student's *t*-test was used to compare differences in the means between groups. *p*-values of less than 0.05 were considered as statistically significant. SPSS 19.0 software (IBM, Chicago, IL, USA) was used for all statistical analyses.

3 Results

3.1 Micro-CT analysis

Characteristics of Ti and CoCrMo particles revealed by scanning electron microscopy are shown in Fig. 1A and B. A mouse calvarial osteolysis model was used to compare the effect of the two types of metal particles *in vivo*. When Ti and CoCrMo particle-stimulated calvariae were evaluated by micro-CT and 3D reconstruction, they showed significant bone resorption as evidenced by surface erosion on the calvariae compared with control calvariae (Fig. 2A). The presence of CoCrMo particles induced more bone loss than that of Ti particles.

Semiquantitative analysis of the bone parameters was consistent with the 3D-reconstructed calvariae. BMD and BV/TV were decreased more strongly in CoCrMo particle-stimulated calvariae than in Ti particle-stimulated calvariae, and were significantly lower in both particle-induced groups than in the control group (Fig. 2B and C). CoCrMo particles induced a markedly greater increase in the number of pores and the total porosity of calvariae than Ti particles (Fig. 2D and E).

3.2 Bone histomorphometry

Histomorphometric analysis also demonstrated that CoCrMo particles induced more marked osteolysis than Ti particles. HE staining showed significantly more extensive erosion of calvarial bone in Ti and CoCrMo particle groups than in the control group (Fig. 3A), but bone erosion was considerably more severe in the CoCrMo particle-exposed group than in the Ti particle-exposed group (Fig. 3B). TRAP staining showed obviously TRAP-positive cells distributed along the eroded bone surface in particle-induced groups compared with the control group (Fig. 3A). Quantitative analysis by micro-CT revealed that OcS/BS was significantly higher in the CoCrMo particle-exposed group than in the Ti particle-exposed group (Fig. 3D), although the numbers of positive cells did not differ significantly between CoCrMo and Ti particle groups (Fig. 3C).

3.3 Expression of osteoclast-specific genes

RT-PCR was used to investigate the effects of the two particles on mRNA expression of osteoclast-specific genes Trap, Ctr, Ck, and nuclear factor of activated T cells c1 (Nfatc1). As shown in Fig. 4, CoCrMo and Ti particles induced significant increases in the mRNA expression of osteoclast-specific genes compared with the control group. In the two particle-exposed groups, CoCrMo particles had a stronger effect than Ti particles to induce expression of Trap (Fig. 4A), Ctr (Fig. 4B), Ck (Fig. 4C), and Nfatc1 (Fig. 4D) mRNAs, and the expression of Trap, Ctr and Nfatc1 differed significantly between the two particle groups.

3.4 RANKL and OPG expression

Considering the importance of the balance between RANKL and OPG in periosteolytic tissue during particle-induced osteolysis, we investigated the effects of the different particles on the

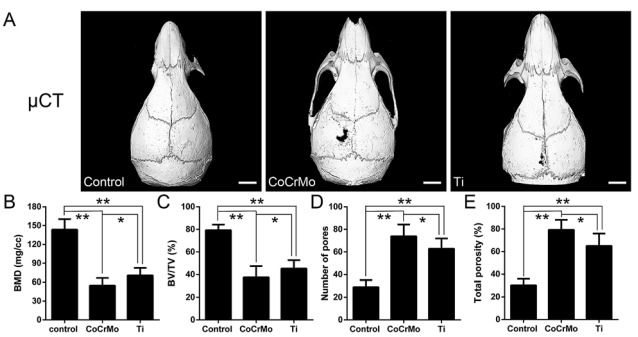

Fig. 2 CoCrMo particles induce greater calvarial osteolysis than Ti particles. (A) Representative micro-CT (μCT) 3D-reconstructed images obtained from each group (scale bar = 5 mm). (B) Bone mineral density (BMD), (C) bone volume/tissue volume ratio (BV/TV), (D) number of pores, and (E) total porosity of each sample were measured within the ROI. $n = 8$ per group, $*p < 0.05$ and $**p < 0.01$.

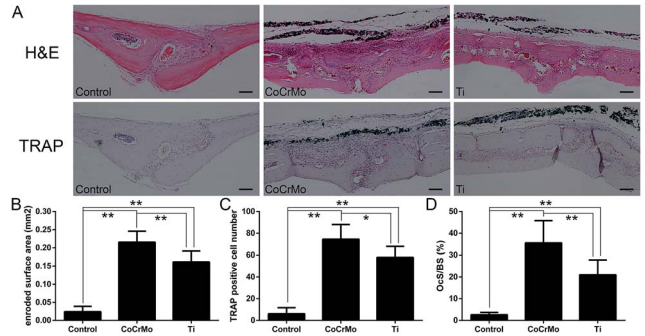

Fig. 3 CoCrMo particles induce more marked bone resorption and osteoclast formation than Ti particles. (A) Hematoxylin and eosin (HE)-, and tartrate-resistant acid phosphatase (TRAP)-stained sections (scale bar = 100 mm). (B) Eroded bone surface (EBS, mm^2), (C) the number of TRAP-positive multinucleated osteoclasts (dark red), and (D) percentage of the osteoclast surface per bone surface (OcS/BS, %) within the ROI were measured in each group. $n = 8$ per group, $*p < 0.05$ and $**p < 0.01$.

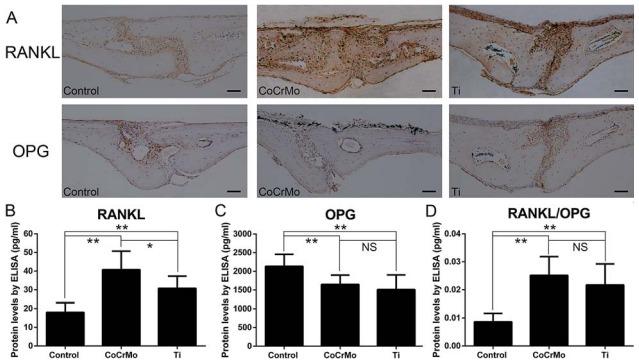

Fig. 5 CoCrMo particles induce a larger RANKL/OPG ratio than Ti particles. (A) Immunohistochemical staining for RANKL and OPG in mouse calvariae of each group (scale bar = 100 μm). ELISAs were performed to determine the protein levels of RANKL (B) and OPG (C) in the media of cultured calvariae. The RANKL/OPG ratio of secreted proteins was also calculated and compared (D). $n = 8$ per group, $*p < 0.05$ and $**p < 0.01$.

expression and secretion of RANKL and OPG. Both CoCrMo and Ti particles induced significant increases in RANKL secretion (Fig. 5B), but significantly reduced OPG secretion relative to the control group (Fig. 5C). Therefore, the ratio of RANKL to OPG was increased markedly in both particle groups compared with the control group (Fig. 5D). However, CoCrMo particles induced a markedly greater increase in RANKL secretion and a slightly smaller reduction in OPG secretion than Ti particles. Therefore, the ratio of RANKL to OPG was slightly higher in CoCrMo particle-exposed tissues.

Consistent with the ELISA results, immunohistochemical staining for RANKL revealed that the two particle groups showed markedly higher production of RANKL and modestly lower expression of OPG than the control group (Fig. 5A). However, positive staining for RANKL was significantly more extensive in the CoCrMo group than in the Ti group, while positive staining for OPG did not show large differences between the two groups.

3.5 Expression of TNF-α, IL-1β, and IL-6

To compare the effects of the two particles on induction of a local inflammatory response, we conducted immunohistochemical staining of the calvarial tissue. The results showed

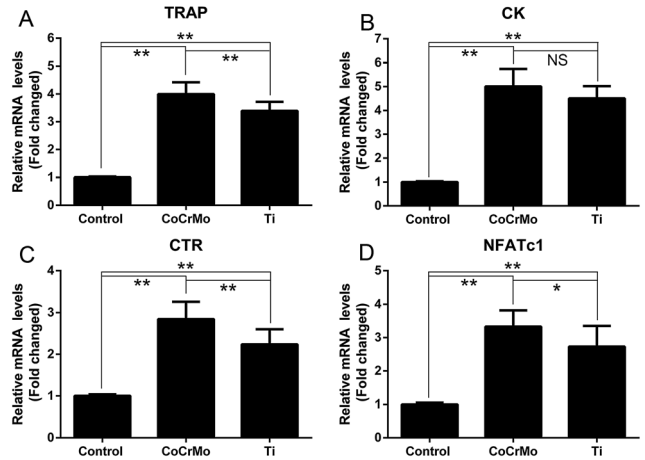

Fig. 4 CoCrMo particles induce more osteoclast-specific gene expression than Ti particles. RT-PCR was used to measure expression of osteoclast-specific genes including (A) TRAP, (B) CK, (C) CTR, and (D) NFATc1. Values are relative to expression in the control group. $n = 8$ per group, $*p < 0.05$ and $**p < 0.01$.

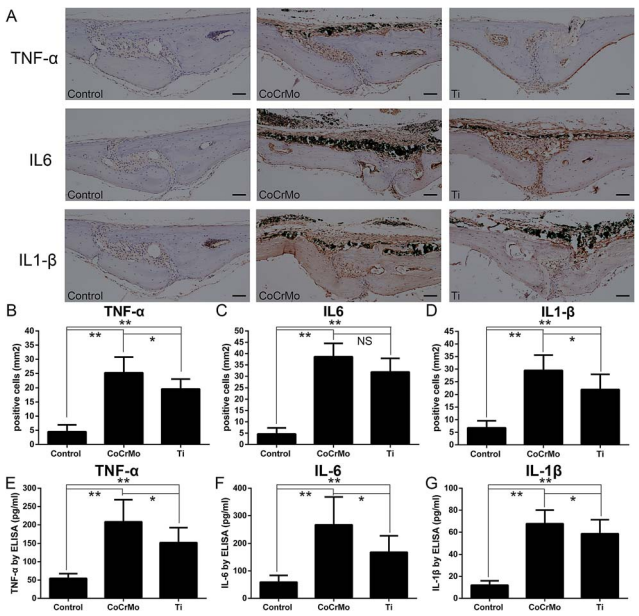

Fig. 6 CoCrMo particles induce a more severe inflammatory response than Ti particles. (A) Immunohistochemical staining for TNF-α, IL-6, and IL-1β in mouse calvariae of each group (scale bar = 100 μm). (B–D) Semiquantitative analysis showed that CoCrMo particles induced more marked inflammatory release of TNF-α (B) and IL-1β (D), but not IL-6 (C), than Ti particles. (E–G) CoCrMo particles lead to significantly more secretion of TNF-α (E), IL-6 (F), and IL-1β (G) into supernatants of cultured Ti particle-stimulated calvariae than Ti particles. $n = 8$ per group, $*p < 0.05$ and $**p < 0.01$.

significantly positive staining for TNF-α, IL-6, and IL-1β in the particle-treated groups (Fig. 6A), which had accumulated around the eroded bone surfaces, compared with the control group. Semiquantitative analysis indicated that the CoCrMo particles induced markedly more cells positive for TNF-α (Fig. 6B) and IL-1β (Fig. 6D), but not IL-6 (Fig. 6C), than Ti particles.

We measured relative proinflammatory cytokine production and secretion of TNF-α, IL-1β, and IL-6 into the media of cultured calvariae. CoCrMo and Ti particles stimulated significant increases in the secretion of proinflammatory cytokines TNF-α (Fig. 6E), IL-1β (Fig. 6F), and IL-6 (Fig. 6G) compared with the control group. CoCrMo particles induced significantly greater increases in the protein levels of TNF-α, IL-6, and IL-1β than Ti particles.

4 Discussion

It has been well documented that the duration of the implantation and joint functions depend greatly on the wear speed of mobile surfaces and the amount of formed wear particles.[6] Therefore, it is necessary to investigate the effects of different particles on periprosthetic osteolysis. Zhang *et al.* investigated the effects of different kinds of implant particles on inflammatory cytokine release by human peripheral blood monocytes, and found that UHMWPE particles induced stronger MCP-1 and IL-6 expression than Ti or CoCrMo particles.[30] Rader *et al.* demonstrated that Co and polyethylene particles had stronger effects on TNF-α expression in macrophages than Ti particles.[31] The effects of each single particle type on inflammatory osteolysis *in vitro* have been investigated repeatedly.[25,26] However, few studies have compared induction of bone resorption by different types of particles *in vivo*. In the present study, we primarily investigated the effects of CoCrMo and Ti particles on the inflammatory response and bone resorption in a mouse calvaria model.

The results of this *in vivo* study confirm that CoCrMo particles induce more severe inflammatory osteolysis, according to micro-CT images and greater release of proinflammatory cytokines TNF-α, IL-6, and IL-1β, than Ti particles. The CoCrMo and Ti particles used in this study had diameters at the micron scale, which are reportedly factors in the induction of inflammatory osteolysis by wear particles. Generally, particles of 0.2–10 μm are bioactive and capable of inducing proinflammatory cytokine release on a mass scale.[13–15] Dalal *et al.* reported that CoCrMo alloy particles were significantly more bioreactive than nearly equal-sized Ti alloy particles by assessing cell viability and proliferation, and were more proinflammatory based on the release of IL-6, TNF-α, IL-1β, and IL-8. These data are consistent with our results,[32] and indicate CoCrMo particles induce a greater inflammatory response and more bone resorption than Ti particles.

Local inflammatory cell infiltration and the release of proinflammatory cytokines play a major role in particle-induced osteolysis. Several studies have reported the potential utility of inhibiting or blocking proinflammatory cytokine release by Chinese medicine, specific inhibitors, or genetic methods to prevent periprosthetic osteolysis and aseptic loosening.[33–35] Dalal *et al.* reported that the highest cytokine responses of macrophages were to CoCrMo alloy (TNF-α and IL-6) and Ti alloy (IL-1β), whereas the highest responses of fibroblasts and osteoblasts were to CoCrMo alloy (IL-6 and TNF-α).[32] In this study, we examined the secretion of proinflammatory proteins from particle-stimulated mouse calvariae by ELISAs, and found that CoCrMo particles induced significantly greater release of TNF-α, IL-6, and IL-1β than Ti particles, which is consistent with the previously reported results. However, immunohistochemical staining showed that expression of IL-6 did not significantly differ between two particle groups. *In vivo*, inflammation is a synergistic result of the reactions of each cell type (including but not limited to osteoblasts, fibroblasts, and macrophages) to CoCrMo and Ti particles.

It is increasingly accepted that the balance between RANKL and OPG plays an important role in osteoclastic osteolysis. RANKL is an activator of NF-κB signaling and accelerates the inflammatory response, whereas OPG is a competitive ligand of the RANKL receptor.[26,29] Geng *et al.* reported that Ti particles significantly increased the expression of RANKL, but reduced the expression of OPG, thus increasing the RANKL/OPG ratio.[29] Our results using Ti particles were similar to those of Geng *et al.*, but CoCrMo particles had a slightly stronger effect on the RANKL/OPG ratio than Ti particles.

The induction of a greater inflammatory response and osteolytic bone loss by CoCrMo particles than Ti particles *in vivo* might be largely due to their intrinsic higher level of capabilities to induce cellular responses. This can be partly explained by the corrosion issues that are a significant concern in CoCrMo-related arthroplasty failure. Studies have indicated that a mass of harmful metallic ions can be released from a CoCrMo implant, even without mechanical abrasion, which aggravates the cellular responses.[36,37] The reported higher cytotoxic effect of CoCrMo particles than that of Ti particles is also highly related to the enhanced release of proinflammatory factors.[38,39] The greater intrinsic inflammation-inducing capability of CoCrMo particles can also be attributed to the more aggressive type of cellular responses they evoke compared with that of Ti particles. The inflammatory response to Ti particles, which is similar to the response to polyethylene particles, is predominantly a chronic inflammatory reaction in which macrophages are mainly activated to release proinflammatory cytokines and differentiate into functional osteoclasts.[40,41] However, *in vivo*, CoCrMo particles not only activate macrophages, but also stimulate T cells of the immune system and activate the inflammasome danger signaling pathway that plays a cooperative role in the inflammatory response.[42,43] In this study, to compare the effects of the different particle types on inducing osteolysis, we applied equal doses (the mass in particular) of particles to each mouse calvaria of particle-stimulated groups, and the sizes of the two particles were of the same magnitude. However, the shapes of the two particles were not consistent and could have some effects on the ability of the particles to induce osteolysis. In addition, the bioactivity of wear particles *in vivo* can also be determined by various other parameters including the zeta-potential, surface chemistry, pH of fluids

containing them, and charges. Thus, further investigations detailing these aspects at cellular or even molecular levels are needed.

5 Conclusions

In summary, our results show that CoCrMo particles had a stronger effect on inducing an inflammatory response and osteolysis than Ti particles in a mouse calvarial model. CoCrMo particles activated more osteoclasts by markedly increasing their expression of specific relevant genes, namely Trap, Ctr, and Nfatc1, and induced a greater degree of inflammatory cytokine release.

Conflicts of interest

There are no conflicts of interest to declare.

Acknowledgements

We gratefully acknowledge the generous assistance and CoCrMo particles provided by Sandvik (Stockholm, Sweden). This work was funded by the Shanghai industry and medicine cooperation project (12DZ1940204). We thank Chongyang Wang, Maimaitiaili Tuerxun, and Yucheng Wang for their kind assistance in this study.

References

1 R. M. Urban, D. J. Hall, C. Della Valle, M. A. Wimmer, J. J. Jacobs and J. O. Galante, *J. Bone Jt. Surg., Am. Vol.*, 2012, **94**, 1877–1885.
2 S. M. Kurtz, E. Lau, K. Ong, K. Zhao, M. Kelly and K. J. Bozic, *Clin. Orthop. Relat. Res.*, 2009, **467**, 2606–2612.
3 K. S. Park, J. K. Seon, K. B. Lee, S. K. Kim, C. K. Chan and T. R. Yoon, *J. Arthroplasty*, 2017, **32**, 503–509.
4 M. Tsukamoto, H. Ohnishi, T. Mori, M. Kawasaki, S. Uchida and A. Sakai, *J. Arthroplasty*, 2017, **32**, 161–165.e1.
5 C. J. Della Valle, N. W. Mesko, L. Quigley, A. G. Rosenberg, J. J. Jacobs and J. O. Galante, *J. Bone Jt. Surg., Am. Vol.*, 2009, **91**, 1130–1135.
6 E. Sukur, Y. E. Akman, Y. Ozturkmen and F. Kucukdurmaz, *Open Orthop. J.*, 2016, **10**, 241–251.
7 C. Nich, Y. Takakubo, J. Pajarinen, M. Ainola, A. Salem, T. Sillat, A. J. Rao, M. Raska, Y. Tamaki, M. Takagi, Y. T. Konttinen, S. B. Goodman and J. Gallo, *J. Biomed. Mater. Res., Part A*, 2013, **101**, 3033–3045.
8 P. E. Purdue, P. Koulouvaris, H. G. Potter, B. J. Nestor and T. P. Sculco, *Clin. Orthop. Relat. Res.*, 2007, **454**, 251–261.
9 C. Alley, W. Haggard and R. Smith, *J. Long Term Eff. Med. Implants*, 2014, **24**, 45–56.
10 J. Gallo, M. Slouf and S. B. Goodman, *J. Biomed. Mater. Res., Part B*, 2010, **94**, 171–177.
11 F. Lebre, R. Sridharan, M. J. Sawkins, D. J. Kelly, F. J. O'Brien and E. C. Lavelle, *Sci. Rep.*, 2017, **7**, 2922.
12 Y. Tabei, S. Sugino, K. Eguchi, M. Tajika, H. Abe, Y. Nakajima and M. Horie, *Biochem. Biophys. Res. Commun.*, 2017, **490**, 499–505.
13 J. B. Matthews, A. A. Besong, T. R. Green, M. H. Stone, B. M. Wroblewski, J. Fisher and E. Ingham, *J. Biomed. Mater. Res.*, 2000, **52**, 296–307.
14 T. R. Green, J. Fisher, J. B. Matthews, M. H. Stone and E. Ingham, *J. Biomed. Mater. Res.*, 2000, **53**, 490–497.
15 T. R. Green, J. Fisher, M. Stone, B. M. Wroblewski and E. Ingham, *Biomaterials*, 1998, **19**, 2297–2302.
16 A. Sabokbar, R. Pandey and N. A. Athanasou, *J. Mater. Sci.: Mater. Med.*, 2003, **14**, 731–738.
17 H. Migaud, S. Putman, G. Kern, R. Isida, J. Girard, N. Ramdane, C. P. Delaunay and M. Hamadouche, *Clin. Orthop. Relat. Res.*, 2016, **474**, 2190–2199.
18 K. J. Bozic, K. Ong, E. Lau, S. M. Kurtz, T. P. Vail, H. E. Rubash and D. J. Berry, *Clin. Orthop. Relat. Res.*, 2010, **468**, 2357–2362.
19 J. A. Keeney, J. M. Martell, G. Pashos, C. J. Nelson, W. J. Maloney and J. C. Clohisy, *Hip Int.*, 2015, **25**, 435–441.
20 M. H. L. Liow and Y. M. Kwon, *Int. Orthop.*, 2017, **41**, 885–892.
21 L. Renner, T. Schmidt-Braekling, M. Faschingbauer and F. Boettner, *Arch. Orthop. Trauma. Surg.*, 2016, **136**, 1657–1662.
22 G. S. Matharu, H. G. Pandit and D. W. Murray, *Clin. Orthop. Relat. Res.*, 2017, **475**, 304–314.
23 P. H. Wooley, R. Morren, J. Andary, S. Sud, S. Y. Yang, L. Mayton, D. Markel, A. Sieving and S. Nasser, *Biomaterials*, 2002, **23**, 517–526.
24 G. Valles, E. Gil-Garay, L. Munuera and N. Vilaboa, *Biomaterials*, 2008, **29**, 2326–2335.
25 Y. P. Zhao, J. L. Wei, Q. Y. Tian, A. T. Liu, Y. S. Yi, T. A. Einhorn and C. J. Liu, *Sci. Rep.*, 2016, **6**, 20909.
26 C. Jiang, F. Xiao, X. Gu, Z. Zhai, X. Liu, W. Wang, T. Tang, Y. Wang, Z. Zhu, K. Dai, A. Qin and J. Wang, *Biochimie*, 2015, **111**, 107–118.
27 T. Sato, J. Pajarinen, T. H. Lin, Y. Tamaki, F. Loi, K. Egashira, Z. Yao and S. B. Goodman, *J. Biomed. Mater. Res., Part A*, 2015, **103**, 3872–3878.
28 Z. Zhai, X. Qu, H. Li, K. Yang, P. Wan, L. Tan, Z. Ouyang, X. Liu, B. Tian, F. Xiao, W. Wang, C. Jiang, T. Tang, Q. Fan, A. Qin and K. Dai, *Biomaterials*, 2014, **35**, 6299–6310.
29 D. Geng, Y. Xu, H. Yang, J. Wang, X. Zhu, G. Zhu and X. Wang, *Biomaterials*, 2010, **31**, 1996–2000.
30 K. Zhang, S. Y. Yang, S. Yang, L. Bai, P. Li, D. Liu, J. R. Schurman II and P. H. Wooley, *J. Biomed. Mater. Res., Part A*, 2015, **103**, 358–364.
31 C. P. Rader, B. Baumann, T. Sterner, O. Rolf, C. Hendrich, N. Schutze and F. Jakob, *Biomed. Tech.*, 1999, **44**, 135–141.
32 A. Dalal, V. Pawar, K. McAllister, C. Weaver and N. J. Hallab, *J. Biomed. Mater. Res., Part A*, 2012, **100**, 2147–2158.
33 L. Peng, H. Wang, K. Song, H. Wang and P. Liu, *Mol. Med. Rep.*, 2016, **13**, 1010–1018.
34 L. Dong, R. Wang, Y. A. Zhu, C. Wang, H. Diao, C. Zhang, J. Zhao and J. Zhang, *J. Orthop. Res.*, 2008, **26**, 1114–1120.

35 B. F. Boyce, P. Li, Z. Yao, Q. Zhang, I. R. Badell, E. M. Schwarz, R. J. O'Keefe and L. Xing, *Keio J. Med.*, 2005, **54**, 127–131.
36 R. H. Oskouei, M. R. Barati, H. Farhoudi, M. Taylor and L. B. Solomon, *Mater. Sci. Eng., C*, 2017, **79**, 390–398.
37 D. J. Hall, R. Pourzal, H. J. Lundberg, M. T. Mathew, J. J. Jacobs and R. M. Urban, *J. Biomed. Mater. Res., Part B*, 2017, DOI: 10.1002/jbm.b.33972.
38 P. Prokopovich, *Adv. Colloid Interface Sci.*, 2014, **213**, 36–47.
39 V. K. Raghunathan, M. Devey, S. Hawkins, L. Hails, S. A. Davis, S. Mann, I. T. Chang, E. Ingham, A. Malhas, D. J. Vaux, J. D. Lane and C. P. Case, *Biomaterials*, 2013, **34**, 3559–3570.
40 S. B. Goodman, E. Gibon, J. Pajarinen, T. H. Lin, M. Keeney, P. G. Ren, C. Nich, Z. Yao, K. Egashira, F. Yang and Y. T. Konttinen, *J. R. Soc., Interface*, 2014, **11**, 20130962.
41 T. H. Lin, Y. Tamaki, J. Pajarinen, H. A. Waters, D. K. Woo, Z. Yao and S. B. Goodman, *Acta Biomater.*, 2014, **10**, 1–10.
42 M. J. Pearson, R. L. Williams, H. Floyd, D. Bodansky, L. M. Grover, E. T. Davis and J. M. Lord, *Biomaterials*, 2015, **67**, 232–239.
43 M. S. Caicedo, R. Desai, K. McAllister, A. Reddy, J. J. Jacobs and N. J. Hallab, *J. Orthop. Res.*, 2009, **27**, 847–854.